Transmission-Line Negative Group Delay Networks With Improved Signal Attenuation

Girdhari Chaudhary, *Member, IEEE*, and Yongchae Jeong, *Senior Member, IEEE*

***Abstract*—This letter presents a novel design and implementation of a transmission-line negative group delay (NGD) network with improved signal attenuation (SA). Theoretical analysis shows that the NGD time can be controlled by characteristic impedance of the coupled line, coupling coefficients, and resistor, respectively. The low SA characteristic in the proposed structure is obtained due to high characteristic impedance of the coupled line. To validate the proposed structure, the transmission-line NGD networks are fabricated and measured at 2.14 GHz. From the experiment, the differential-phase group delay (GD) time and SA for a single stage are -6.16 ns and 8.65 dB over bandwidth of 15 MHz, respectively. For bandwidth enhancement, two-stage NGD networks with slightly different center frequencies are designed and fabricated, where GD of -7.48 ± 0.84 ns and SA of 17.45 dB were obtained over a bandwidth of 28 MHz.**

***Index Terms*—Coupled line, dispersion engineering, negative group delay network, transmission line.**

I. Introduction

In RECENT years, there has been a great deal of interest in designing negative group delay (NGD) networks at microwave frequencies. The NGD is equivalent to an increasing phase with frequency within a limited frequency bandwidth [1]–[5]. The interesting characteristics of NGD networks have been applied to various practical application in communication systems such as shortening or reducing delay lines, enhancing the efficiency of feedforward linearization amplifier, and minimizing the beam-squint in phased array antenna systems, respectively [6]–[10]. Recently, new and interesting application of NGD networks has been reported in realization of non-Foster reactive elements such as negative capacitances or inductances [11]. The major drawback of previously presented NGD networks was their inherent signal attenuation (SA); this can be resolved by a gain compensation amplifier with the expense of increased noise due to out-of-band gain and other tradeoffs (such as stability problems).

A few works have been performed regarding the improved SA of NGD network. In [12], a composite NGD network with smaller signal attenuation is presented. However, this circuit requires parallel lumped elements (such as capacitors and inductors) between two transmission lines that make implementation difficulty at microwave frequencies. The distributed line NGD network with improved SA is presented in [13]. However, it is also difficult to further improve the SA because of realization difficulty of transmission line with characteristic impedance higher than 140 Ω in printed circuit board (PCB) technology.

In this letter, a design of an NGD network with low SA is presented. The low SA characteristic is possible due to high characteristic impedance of the coupled line. For bandwidth extension, two NGD networks with slightly different frequencies are cascaded and measured.

Manuscript received February 23, 2014; revised April 09, 2014; accepted April 25, 2014. Date of publication May 29, 2014; date of current version June 11, 2014. This work was supported by the Basic Science Research Program through the National Research Foundation of Korea (NRF) funded by the Ministry of Science, ICT and Future Planning (2013006660).

The authors are with the Division of Electronics Engineering, IT Convergence Research Center, Chonbuk National University, Jeonju 561-756, Korea (e-mail: ycjeong@jbnu.ac.kr).

Color versions of one or more of the figures in this letter are available online at http://ieeexplore.ieee.org.

Digital Object Identifier 10.1109/LAWP.2014.2327098

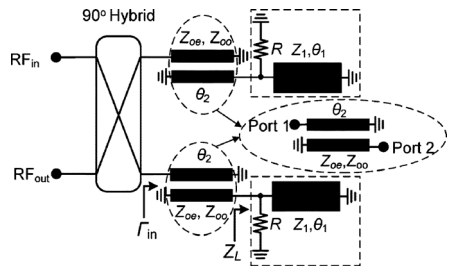

Fig. 1. Proposed structure of transmission line NGD network.

II. Mathematical Analysis

The proposed reflection-type NGD network is shown in Fig. 1; it consists of a 3-dB hybrid coupler, coupled lines, resistors R, and transmission lines with characteristic impedance Z_1 and electrical length θ_1. For the purpose of finding voltage reflection coefficient ($\Gamma_{\rm in}$) of the reflection termination of proposed structure, the Y-parameter of the coupled line with short-circuited through and coupling ports [14]–[16], as shown in Fig. 1, is given as

$$[Y] = \begin{bmatrix} -j\frac{Y_{0e}+Y_{0o}}{2}\cot\theta_2 & -j\frac{Y_{0o}-Y_{0e}}{2}\csc\theta_2 \\ -j\frac{Y_{0o}-Y_{0e}}{2}\csc\theta_2 & -j\frac{Y_{0e}+Y_{0o}}{2}\cot\theta_2 \end{bmatrix} \quad (1)$$

where $Z_{0e} = 1/Y_{0e}, Z_{0o} = 1/Y_{0o}, \theta_2$ are the even- and odd-mode impedances and electrical length of coupled lines, respectively. Furthermore, when an isolation port 2 is terminated with a load $Z_L = 1/Y_L$, the input impedance of coupled line is given as

$$Y_{\rm in} = Y_{11} - \frac{Y_{12}Y_{21}}{Y_{22}+Y_L}. \quad (2)$$

Assuming frequency-dependent electrical length $\theta_1 = \theta_2 = \theta = \pi f/2f_0$, the input voltage reflection coefficient with port impedance $Z_0 = 1/Y_0$ is given as

$$|\Gamma_{\rm in}|\angle\phi = \sqrt{\frac{X_1^2+X_2^2}{X_3^2+X_4^2}}\angle\tan^{-1}\left(\frac{X_2}{X_1}\right) + \tan^{-1}\left(\frac{X_4}{X_3}\right) \quad (3)$$

where f and f_0 are operating and design center frequency, respectively. The values of X_1, X_2, X_3, and X_4 are given as

$$X_1 = Y_0 G - B^2 \csc^2(\pi f/2f_0) + A(Y_1 + A)\cot^2(\pi f/2f_0) \tag{4a}$$

$$X_2 = [AG - Y_0(Y_1 + A)]\cot(\pi f/2f_0) \tag{4b}$$

$$X_3 = Y_0 G + B^2 \csc^2(\pi f/2f_0) - A(Y_1 + A)\cot^2(\pi f/2f_0) \tag{4c}$$

$$X_4 = [AG + Y_0(Y_1 + A)]\cot(\pi f/2f_0). \tag{4d}$$

The values of A, B, G, and Y_1 are given as

$$A = \frac{Y_{0e} + Y_{0o}}{2} = \frac{1}{Z_c C_{\text{eff}}} \quad B = \frac{Y_{0o} - Y_{0e}}{2} = \frac{1}{Z_c}$$
$$G = \frac{1}{R} \quad Y_1 = \frac{1}{Z_1} \tag{5a}$$

$$Z_c = \frac{2Z_{0e}}{Z_{0e}/Z_{0o} - 1} = Z_{0e}\frac{1 - C_{\text{eff}}}{C_{\text{eff}}} = Z_{0o}\frac{1 + C_{\text{eff}}}{C_{\text{eff}}} \tag{5b}$$

where Z_c and C_{eff} are the equivalent characteristic impedance and coupling coefficient of the coupled line [14]–[16], respectively. As seen from (5b), very high characteristic impedance Z_c can be obtained if the ratio of Z_{0e} to Z_{0o} close to unity or C_{eff} becomes very small [14]–[16]. Therefore, the differential-phase group delay (GD) of the reflection termination of the proposed structure for frequency dependent electrical length can be obtained as

$$\tau = -\frac{d\phi}{d\omega} = -\frac{d\angle\Gamma_{\text{in}}}{d\omega} = \frac{X_2 X_1' - X_1 X_2'}{X_1^2 + X_2^2} + \frac{X_4 X_3' - X_3 X_4'}{X_3^2 + X_4^2} \tag{6}$$

where

$$X_1' = -X_3' = \frac{1}{2f_0} \times [B^2 - A(Y_1 + A)]\csc^2(\pi f/2f_0)\cot(\pi f/2f_0) \tag{7a}$$

$$X_2' = -\frac{1}{2f_0}[AG - Y_0(Y_1 + A)]\csc^2(\pi f/2f_0) \tag{7b}$$

$$X_4' = -\frac{1}{2f_0}[AG + Y_0(Y_1 + A)]\csc^2(\pi f/2f_0). \tag{7c}$$

Therefore, the maximum SA and GD of the proposed structure at f_0 are obtained as

$$|\Gamma_{\text{in}}|_{f=f_0} = \left|\frac{Z_c^2 - Z_0 R}{Z_c^2 + Z_0 R}\right| \tag{8}$$

$$\tau|_{f=f_0} = -\frac{Z_0 Z_c\left(R^2 Z_1 + R^2 Z_c C_{\text{eff}} - Z_c^2 Z_1\right)}{2f_0 Z_1 C_{\text{eff}}\left(Z_c^4 - Z_0^2 R^2\right)} \tag{9}$$

where Z_0 is the termination port impedance. As seen from (8), the maximum SA at f_0 depends on Z_c and R. Similarly, the GD time is a function of R, Z_1, Z_c, and C_{eff}. For better understanding of expressions (8) and (9), the calculated maximum achievable GD, SA, and R for different values of Z_c and C_{eff} are shown in Fig. 2. In this case, the value of Z_1 is fixed as 20 Ω. As seen from these figures, the predefined GD time with low SA can be obtained with high value of Z_c. Moreover, the slight improvement in SA is also seen due to decreasing value of C_{eff}.

Fig. 3 shows the simulated results of the GD and SA characteristics for different values of Z_c and R with fixed maximum achievable GD of -6 ns at $f_0 = 2.14$ GHz. As seen in these figures, the improved SA characteristic can be obtained with high value of Z_c. However, the NGD bandwidth is decreased. In order to investigate the relation between SA and NGD bandwidth, the NGD bandwidth (NGD BW $= f_2 - f_1$) is defined as the bandwidth of GD of 0 ns as shown in Fig. 3 for convenience.

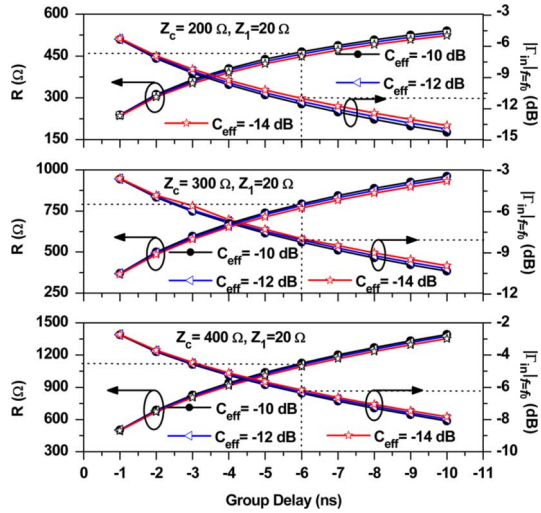

Fig. 2. Calculated maximum achievable NGD time, $|\Gamma_{\text{in}}|$ at $f = f_0$ and R for different Z_c and C_{eff} with $Z_1 = 20\ \Omega$.

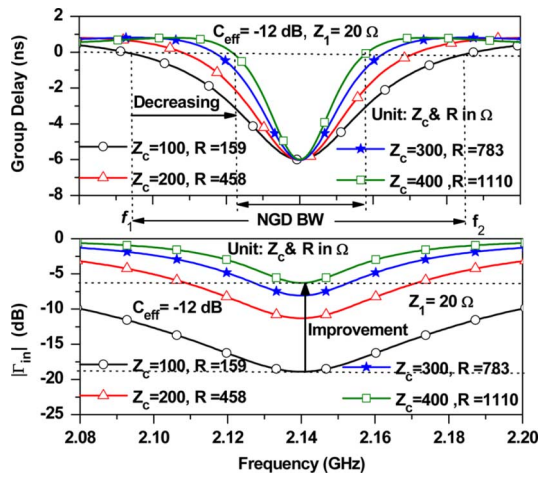

Fig. 3. Calculated group delay and magnitude ($|\Gamma_{\text{in}}|$) characteristics for different Z_c and R with fixed maximum achievable NGD time of -6 ns at f_0 with $Z_1 = 20\ \Omega$ and $C_{\text{eff}} = -12$ dB.

Fig. 4 shows the calculated the NGD bandwidths and maximum achievable SA characteristics for different values of maximum achievable NGD time at f_0. When Z_c is increased toward high value; the SA and NGD bandwidth are decreased. Therefore, there is a trade-off between improved SA and NGD bandwidth.

In order to compare the performance of the proposed structure to conventional transmission-line NGD networks, the circuit parameters of these networks are given in Table I for the maximum achievable GD $= -6$ ns and SA $= 8.26$ dB at $f_0 = 2.14$ GHz. For fair comparison, the same GD and bandwidth at the same center frequency are assumed for the conventional and proposed structures. As seen from this table, the circuit parameters of conventional transmission-line NGD networks [2], [9], [10], and [13] are practically unrealizable values due to very high or low

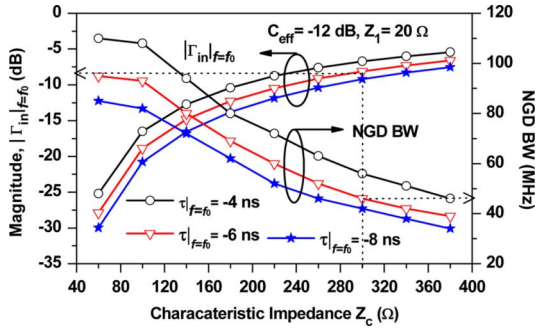

Fig. 4. Calculated maximum magnitude $|\Gamma_{in}|$ at $f = f_0$ and NGD bandwidth for different Z_c with $C_{eff} = -12$ dB and $Z_1 = 20\ \Omega$.

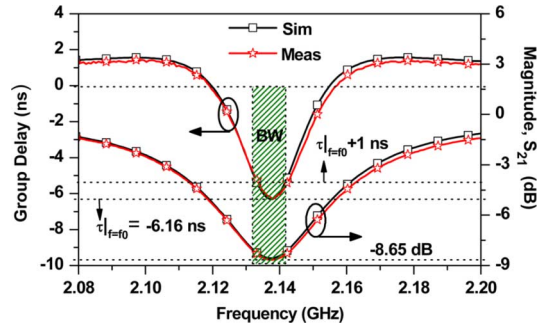

Fig. 5. Simulation and measurement results of the single-stage NGD network.

TABLE I
CIRCUIT PARAMETERS OF THE CONVENTIONAL TRANSMISSION-LINE NGD NETWORKS FOR GD $= -6$ ns AND SA $= 8.26$ dB AT $f_0 = 2.14$ GHz

Transmission line NGD networks								Ref.
Configurations	R (Ω)	Z_C (Ω)	R_2 (Ω)	L (nH)	C (pF)	Z_1 (Ω)	Z_2 (Ω)	
R, λ/4, Z_C	15.74	1317.37						[2]*
R, λ/2, Z_C	15.74	658.68						[2]*
R, λ/4, Z_C	112.96	5269.96						[9]** [10]**
R, λ/2, Z_C	112.96	2634.98						
R, λ/4, Z_C	22.13	0.4715						
R, λ/2, Z_C	22.13	0.9431						
R_2, Z_1, C, L, Z_2, λ/8, λ/8	79		50	0.08832	61.8820	50	50	[12]**
Z_1, R, Z_2, λ/4, λ/4	199.18					150	4.32	[13]**

*= Transmission type, **=Reflection type

characteristic impedance of the line, which required very narrow or wide width of the transmission line. Even though the practical realizable values of characteristic impedance of the line are available in case of the composite NGD network [12], it is difficult to implement at microwave frequencies due to the use of lumped elements between the two transmission lines. Moreover, it is also possible to get the same characteristics as the proposed structure with conventional lumped element (LE)-type NGD networks [2]–[6], [9], [10], but it is difficult to implement these networks at microwave frequencies.

III. SIMULATION AND MEASUREMENT RESULTS

To validate the proposed structure experimentally, a microstrip-line NGD network was designed for the GD -6.5 ns at the operating center frequency (f_0) of 2.14 GHz and fabricated on the substrate with a dielectric constant (ε_r) of 2.2 and a thickness (h) of 31 mil. For the 3-dB hybrid coupler, a quadrature surface-mount hybrid coupler S03A2500N1 from Anaren was used. The circuit parameter values of the designed NGD network are $Z_c = 300\ \Omega$, $Z_{0e} = 138.74\ \Omega$, $Z_{0o} = 71.95\ \Omega$, $C_{eff} = -10$ dB, $Z_1 = 20\ \Omega$, and $R = 820\ \Omega$, respectively. The electrical lengths of coupled lines and short-circuited transmission line are 90° at 2.14 GHz. The coupled lines are meandered in order to reduce the circuit size. The simulation and measurement results of the single-stage NGD network are shown in Fig. 5. As seen from

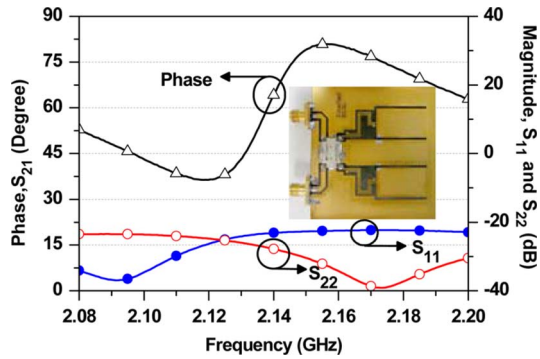

Fig. 6. Measured input/output return losses, phase response, and photograph of fabricated circuit.

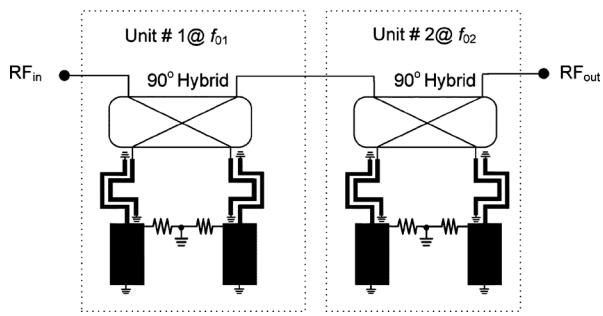

Fig. 7. Cascaded two NGD networks with slightly different center frequencies for NGD bandwidth enhancement.

the figure, the measurement results are in good agreement with the simulation results. The measured GD and SA at 2.14 GHz are -6.16 ns and 8.65 dB, respectively.

Fig. 6 shows the measured input/output return losses and the transmission phase response for single-stage NGD network. The measured return losses are better than 22 dB. A photograph of the fabricated NGD network is shown in Fig. 6.

One way to enhance the NGD bandwidth is to cascade NGD networks with slightly different center frequencies [2], [6], [9]. For this purpose, two different NGD networks are designed for GD time of -8.50 ns at center frequencies $f_{01} = 2.128$ GHz and $f_{02} = 2.154$ GHz, respectively, as shown in Fig. 7. Therefore, circuit parameters of each NGD networks are the same as previously, except the R values, which are given as 910 Ω for both units of NGD networks.

The measurement and simulation results of cascaded two NGD networks are given in Fig. 8. The measurement results are good agreement with simulation. As seen in this figure, the maximum achievable NGD time and SA are obtained as -7.48 ± 0.84 ns and 17.45 dB at center frequency 2.145 GHz,

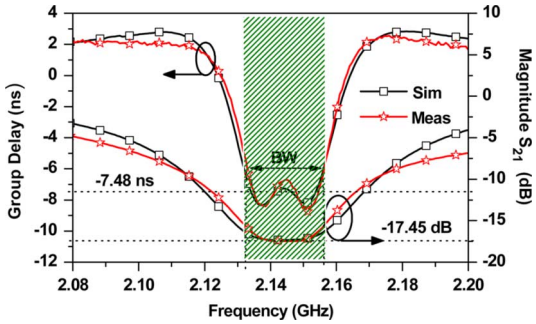

Fig. 8. Simulation and measurement results of cascaded two NGD networks.

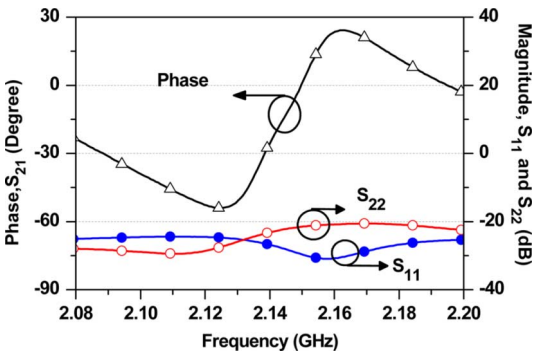

Fig. 9. Measured input/output return losses and phase response of fabricated cascaded circuit.

TABLE II
PERFORMANCE COMPARISON

	f_0 (GHz)	GD_{max} (ns)		SA_{max} (dB)		GD_{max}± 1ns BW (MHz)	For R±5% variation	
		I	II	I	II		ΔGD (ns)	ΔSA (dB)
[4]-[5]	1.00	-10	x	30	x	x	x	x
[6]	0.55	-6.0	x	x	x	x	x	x
[9]-[10]	2.14	-9.0	-9.0	33.1	64.2	35	>46	>23.9
[12]*	2.14	-6.7	x	14.3	x	18	<2.2	<2.3
[13]	2.14	-7.9	x	16.5	x	15	<2.8	<2.9
This work	**2.14**	**-6.16**	**-7.48**	**8.65**	**17.45**	**28**	**<1.7**	**<1.0**

I = single unit NGD network
II = cascaded two NGD networks
BW = maximum achievable group delay±1ns bandwidth
ΔGD = change in group delay from reference value
ΔSA = change in signal attenuation from reference value
* = consists of lumped element parallel (R,L,C) in between transmission lines

respectively. The SA can be easily compensated by general-purpose gain amplifiers. When compared to single-stage results presented in Fig. 5, the two-stage NGD network had wider NGD bandwidth than single-stage, showing practical applicability.

Fig. 9 shows the measured input and output return losses and the transmission phase response for two-stage NGD network. The measured return losses are better than 20 dB. As seen in this figure, the slope of the phase is positive over a certain region. This positive phase slope parameter can be used to cancel out the negative phase slope to obtain zero GD or phase compensated response. The performance comparison of the proposed structure is summarized in Table II. As seen in this table, the proposed NGD network has low SA and least performance degradation due to the resistance variation as compared to previous works. Due to improvement SA, the burden of gain amplifiers as well as out-of-band noise can be reduced and can provide the stable operation when it is integrated with the RF system.

IV. CONCLUSION

In this letter, we demonstrate a microstrip-line negative group delay circuit with improved signal attenuation using a high-impedance transmission line. A very high-impedance line is realized with a coupled line in PCB technology without any fabrication difficulty. The improvement in signal attenuation is obtained due to high characteristic impedance of the coupled line. In order to enhance the negative group delay bandwidth, two-stage negative group delay network is designed and fabricated. The negative group delay bandwidth of two-stage network is wider than single-stage, showing the practical applicability in communication systems. Moreover, the low signal attenuation of the proposed circuit helps to reduce the burden of the gain amplifier block. Compared to the conventional circuit, the proposed circuit is less sensitive to resistance variation.

REFERENCES

[1] B. Ravelo, A. Perennec, M. L. Roy, and Y. G. Boucher, "Active microwave circuit with negative group delay," *IEEE Microw. Wireless Compon. Lett.*, vol. 17, no. 12, pp. 861–863, Dec. 2007.
[2] C. D. Broomfield and J. K. A. Everard, "Broadband negative group delay networks for compensation of microwave oscillators and filters," *Electron. Lett.*, vol. 36, no. 23, pp. 1931–1932, Nov. 2000.
[3] M. Kandic and G. E. Bridges, "Bilateral gain-compensated negative group delay circuit," *IEEE Microw. Wireless Compon. Lett.*, vol. 21, no. 6, pp. 308–310, Jun. 2011.
[4] S. Lucyszyn and I. D. Robertson, "Analog reflection topology building blocks for adaptive microwave signal processing applications," *IEEE Microw. Theory Tech.*, vol. 43, no. 3, pp. 601–611, Mar. 1995.
[5] S. Lucyszyn, I. D. Robertson, and A. H. Aghvami, "Negative group delay synthesizer," *Electron. Lett.*, vol. 29, no. 9, pp. 798–800, Apr. 1993.
[6] H. Noto, K. Yamauchi, M. Nakayama, and Y. Isota, "Negative group delay circuit for feed-forward amplifier," in *IEEE Int. Microw. Symp. Dig.*, Jun. 2007, pp. 1103–1106.
[7] B. Ravelo, M. L. Roy, and A. Perennec, "Application of negative group delay active circuits to the design of broadband and constant phase shifters," *Microw. Optical Technol. Lett.*, vol. 50, no. 12, pp. 3078–3080, Dec. 2008.
[8] S. S. Oh and L. Shafai, "Compensated circuit with characteristics of lossless double negative materials and its application to array antennas," *Microw., Antennas Propag.*, vol. 1, no. 1, pp. 29–38, Feb. 2007.
[9] H. Choi, Y. Jeong, C. D. Kim, and J. S. Kenney, "Efficiency enhancement of feedforward amplifiers by employing a negative group delay circuit," *IEEE Trans. Microw. Theory Tech.*, vol. 58, no. 5, pp. 1116–1125, May 2010.
[10] H. Choi, Y. Jeong, C. D. Kim, and J. S. Kenney, "Bandwidth enhancement of an analog feedback amplifier by employing a negative group delay circuit," *Prog. Electromagn. Res.*, vol. 105, pp. 253–272, 2010.
[11] H. Mirzaei and G. V. Eleftheriades, "Realizing non-Foster reactive elements using negative group delay networks," *IEEE Trans. Microw. Theory Tech.*, vol. 61, no. 12, pp. 4322–4332, Dec. 2013.
[12] H. Choi *et al.*, "A design of composite negative group delay circuit with lower signal attenuation for performance improvement of power amplifiers linearization technique," in *IEEE Int. Microw. Symp. Dig.*, Jun. 2011, pp. 1–4.
[13] G. Chaudhary and Y. Jeong, "Distributed transmission line negative group delay circuit with improved signal attenuation," *IEEE Microw. Wireless Compon. Lett.*, vol. 24, no. 1, pp. 20–22, Jan. 2014.
[14] H. R. Ahn and B. Kim, "Small wideband coupled-line ring hybrids with no restriction on coupling power," *IEEE Trans. Microw. Theory Tech.*, vol. 57, no. 7, pp. 1806–1817, Jul. 2009.
[15] H. R. Ahn and S. Nam, "Wideband coupled-line microstrip filters with high-impedance short-circuited stubs," *IEEE Microw. Wireless Compon. Lett.*, vol. 21, no. 11, pp. 586–588, Nov. 2011.
[16] H. R. Ahn, *Asymmetric Passive Components in Microwave Integrated Circuits*. Hoboken, NJ, USA: Wiley, 2006.